Palaeogeography, Palaeoclimatology, Palaeoecology 485 (2017) 293–304

Contents lists available at ScienceDirect

Palaeogeography, Palaeoclimatology, Palaeoecology

journal homepage: www.elsevier.com/locate/palaeo

Multiple generations of buried cold-water coral mounds since the Early-Middle Pleistocene Transition in the Atlantic Moroccan Coral Province, southern Gulf of Cádiz

Vandorpe T.[a,b,*], Wienberg C.[c], Hebbeln D.[c], Van den Berghe M.[a], Gaide S.[c], Wintersteller P.[c], Van Rooij D.[a]

[a] Ghent University, Department of Geology, Renard Centre of Marine Geology, Campus Sterre S8, Krijgslaan 281, 9000 Ghent, Belgium
[b] VLIZ – Flanders Marine Institute, Wandelaarkaai 7, 8400 Oostende, Belgium
[c] MARUM – Center for Marine Environmental Sciences, Bremen University, Leobener Strasse, 28359 Bremen, Germany

ARTICLE INFO

Article history:
Received 4 November 2016
Received in revised form 8 June 2017
Accepted 15 June 2017
Available online 20 June 2017

Keywords:
Glacial
Sediment input
Bottom currents
Early-Middle Pleistocene transition

ABSTRACT

Cold-water coral mounds are common seabed features in the North Atlantic Ocean, where they are mainly restricted to water depths between 200 m and 1000 m. Coral mounds consist of coral fragments and hemipelagic sediments, reflecting an often complex history of mound aggradation and erosion linked to coral vitality. In the southern Gulf of Cádiz along the Moroccan margin, a large field (extension: 1800 km^2) of 781 comparatively small buried and exposed mounds (average height: about 20 m) has recently been discovered. The mounds in the so-called Atlantic Moroccan Coral Province (AMCP) initiated on at least ten different horizons, all of them most likely related to glacial periods since the Early-Middle Pleistocene Transition. A strong link between the intensification of bottom currents and the number of coral mounds rooting on each of the identified horizons is assumed. Also a shift of the average water depth at which coral mounds initiated towards deeper regions and an accompanied increase in mound height is observed between MIS 14 and MIS 12. Finally, reduced or low sediment input is regarded as one of the main factors causing the rather small size of coral mounds in the AMCP in comparison to other Atlantic mound provinces.

1. Introduction

During the last 15 years, cold-water coral (CWC) research experienced a boost resulting in a steadily increasing knowledge regarding their environmental requirements and preferences, their ecology and physiology, their recent spatial distribution and their temporal occurrence (Freiwald, 2002; Freiwald and Roberts, 2005; Hebbeln et al., 2016; Roberts et al., 2006). Of particular interest are framework-forming scleractinian CWC, such as *Lophelia pertusa* and *Madrepora oculata*, as they have the capability to form small to large reefs (Roberts et al., 2006), possibly leading to the development of huge CWC mounds (hereafter called coral mounds; de Haas et al., 2009; Mienis et al., 2006; van Weering et al., 2003). The temporal development of coral mounds often is discontinuous with recurring periods of CWC colonization and mound aggradation alternating with periods of coral demise and possible mound erosion (Roberts et al., 2006; Wienberg and Titschack, 2017). Coral mounds are the result of an interplay between sustained phases of CWC growth and concurrent sediment input, with the sediments being entrapped within the coral framework (known as baffling effect; Huvenne et al., 2009; Titschack et al., 2009) and thus stabilizing the biogenic construction. Over time, this can result in mound aggradation rates of up to 1500 cm kyr^{-1} as calculated for Norwegian coral mounds (Titschack et al., 2015). During periods of coral demise, the mounds might by covered solely by (hemi) pelagic sediments, which later on may act as a weak layer and could induce slumping, widening the mound at the base (Eisele et al., 2008).

Coral mounds are widely distributed in the North Atlantic Ocean, where they occur on the shelf and along the continental margin mainly being confined to water depths of 200 to 1000 m (Roberts, 2009; Wienberg and Titschack, 2017). They can become rather high (tens to hundreds of meters), as for example in the Porcupine Seabight and the Rockall Trough (De Mol et al., 2002; Eisele et al., 2008; Huvenne et al., 2003; Mienis et al., 2006) or remain rather small (several to tens of meters high) as seen for the Moira mounds in the Porcupine Seabight (Wheeler et al., 2007) and along the Moroccan margin (Foubert et al., 2008; Wienberg et al., 2009). Due to their highly heterogeneous composition, the internal structure of coral mounds appears as acoustically transparent on seismic profiles (Hebbeln et al., 2016; Huvenne et al.,

* Corresponding author at: VLIZ – Halve Maan Site, Slipwaykaai 2, 8400 Oostende, Belgium.
E-mail address: thomas.vandorpe@vliz.be (T. Vandorpe).

http://dx.doi.org/10.1016/j.palaeo.2017.06.021
0031-0182/

2007; Pirlet et al., 2010). The dimensions of the coral mounds depend on environmental controls and sediment input. Environmental control for mound aggradation first and foremost depends on a complex set of suitable environmental conditions that allow the CWC themselves to settle, grow and develop into large thriving reefs. Important are distinct ranges for seawater temperature (−1.8 °C to 14.9 °C), salinity (31.7–38.8) and dissolved oxygen concentration (3–7.2 ml l^{-1}) as well as a high net primary production (Davies and Guinotte, 2011; Davies et al., 2008). Additionally, several other chemical and biological parameters such as the pH, the aragonite saturation state and concentrations of dissolved and particulate organic matter were indicated to play an important role in the occurrence of CWC (Davies and Guinotte, 2011; Davies et al., 2008). Given that the physical setting fits the CWC requirements, the availability of sufficient food particles and distinct hydrodynamic processes (geostrophic currents, local bottom currents, internal waves and tides) to deliver the food particles to the corals or enrich food around them (nepheloid layers) are the most important parameters (Hebbeln et al., 2016; Mienis et al., 2007; Mienis et al., 2012). Even under erosive conditions for the surrounding areas, coral mounds can still aggrade (Thierens et al., 2013) as sediments delivered by vigorous bottom currents are entrapped or baffled within the coral framework (Hebbeln et al., 2016; Huvenne et al., 2009; Titschack et al., 2009).

The current knowledge obtained for coral mounds largely originates from examples which have today an exposed position at the seabed surface. However, also buried coral mounds have been discovered along the Moroccan, Mauritanian and Irish margins and in the western Mediterranean Sea (Colman et al., 2005; Foubert et al., 2008; Huvenne et al., 2009; Lo Iacono et al., 2014; Vandorpe et al., 2016). There seem to be some apparent differences between the above mentioned areas regarding the initiation and development of these mounds. For example, the Irish buried mounds of the Magellan mound province, Porcupine Seabight, nearly all root on one single horizon (Huvenne et al., 2007), while hundreds of small coral mounds were identified to have originated at multiple horizons along the Moroccan margin (Foubert et al., 2008; Hebbeln et al., 2015). However, the existing knowledge on buried mounds along the Moroccan margin was so far restricted to a rather small area within and south of the El Arraiche mud volcano province (Fig. 1). As the number of discovered exposed coral mounds along the Moroccan margin increased steadily with every new mapping survey (by now comprising a very large area bordered by the El Arraiche mud volcano province in the north and the SWIM 2 fault in the south; henceforth be called the Atlantic Moroccan Coral Province, AMCP), it is to be expected that also many more buried mounds are present in the area then assumed so far.

The recent knowledge about the temporal development of the Moroccan coral mounds is based on datings of CWC fragments, obtained from gravity cores of exposed coral mounds developed on top of the Pen Duick escarpment and Renard Ridge (Fig. 1), which indicated that mound aggradation was largely restricted to glacial periods during the last 500 kyr (Frank et al., 2011; Wienberg et al., 2009; Wienberg et al., 2010). So far, nothing is known about the timing of the formation of the buried coral mounds in the AMCP. However, the buried mounds are present at several depth levels in the vicinity of sediment drift systems, these provide an initial chronostratigraphic framework (Vandorpe et al., 2016), which allow an appraisal of the temporal evolution of the buried coral mounds possibly going back further in time than the past 500 kyr and indicating when mound formation initiated in this region. Additionally, a thorough evaluation of the number of buried mounds being present in the AMCP as well as of their spatial distribution and dimensions (height, volume) is still lacking. These quantitative data might shed new insights on the spatial occurrence pattern of coral

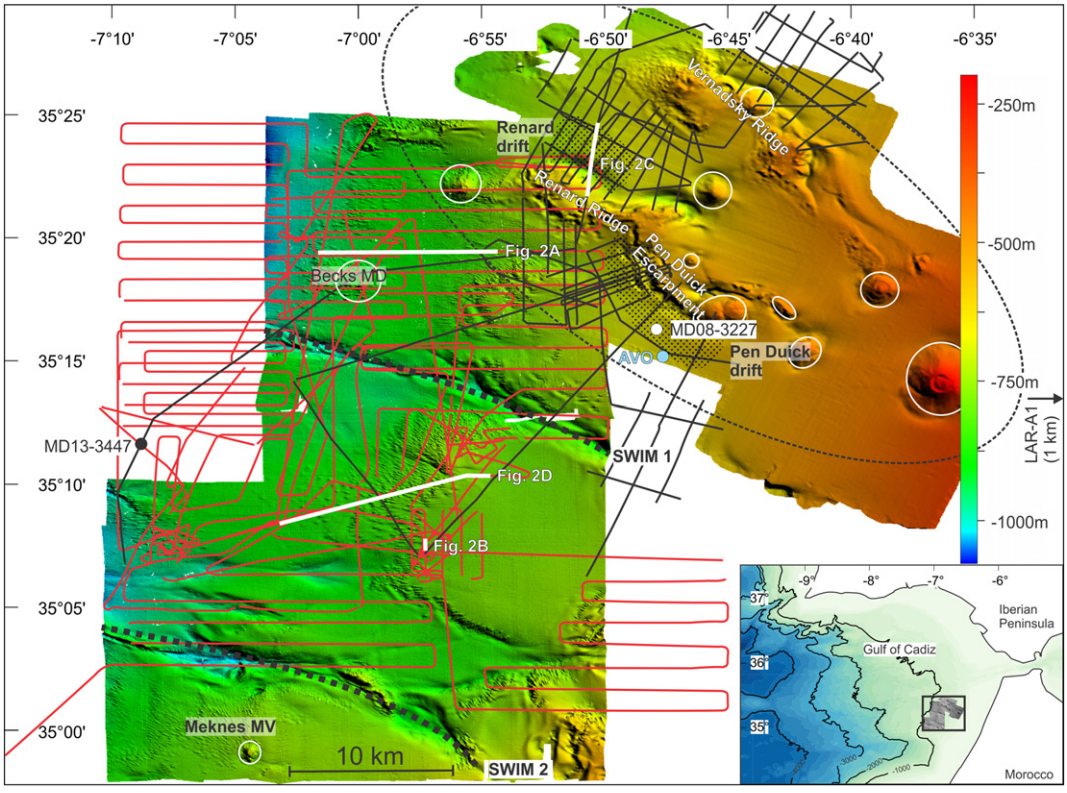

Fig. 1. Multibeam bathymetric map of the study area along the Atlantic Moroccan margin (see overview map in the lower right inset). The PARASOUND profiles are indicated in red and the single channel sparker reflection seismic profiles in black. The Pen Duick and Renard drifts are indicated by the dotted areas. The extent of the El Arraiche mud volcano province (Vandorpe et al., 2016) is indicated by the thin black dashed oval. The location of the amplitude versus offset (AVO) experiment is indicated by the light blue dot, while the core locations of the Marion Dufresne cores are indicated in white/black. The white bold lines indicate the position of seismic profiles displayed in Fig. 2. MD: mud diapir, MV: mud volcano, SWIM: Southwestern Iberian Margin faults.

mounds in the AMCP and improve our understanding of their link with the sedimentary environment, especially since the newly obtained PARASOUND sub-bottom profiler and sparker single channel reflection seismic data (Fig. 1) provide an improved spatial coverage of the seismic lines in the AMCP. Combing the results of the analysis of the spatial distribution and temporal evolution of the coral mounds in the AMCP may significantly improve our understanding on the development of coral mounds in a given region alternating between periods of mound aggradation and stagnation in relation to the sedimentary environment and climate change. Additionally, the discovery of this coral mound province, combined with the continuous discovery of new coral mound settings (Glogowski et al., 2015; Matos et al., 2015; Ross et al., 2017), may shed new light on the enormous scale of carbonate deposition along the intermediate depths of the Atlantic margin.

2. Regional setting

The southern Gulf of Cádiz along the northern Atlantic Moroccan margin was influenced by several phases of rifting, compression and extension since the Triassic and is still influenced by the ongoing African-Eurasian convergence which resulted in the emplacement of a large allochthonous unit (Maldonado et al., 1999; Medialdea et al., 2004). The study area lies on top of the southern part of this large allochthonous

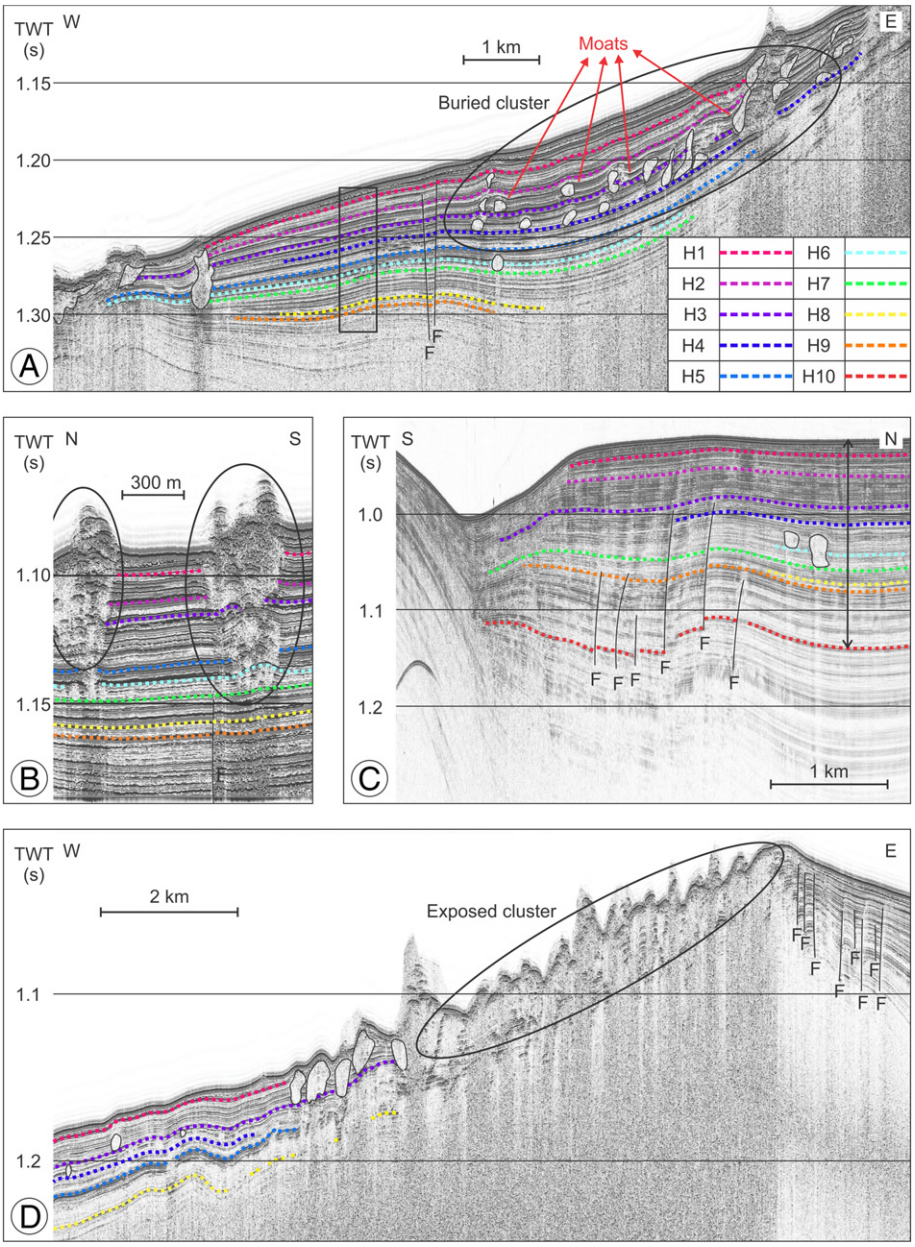

Fig. 2. Seismic profiles (for position see Fig. 1) with all depths indicated in seconds two-way-travel times. A. PARASOUND profile extending from the Becks mud diapir towards the Renard Ridge showing nine (H1-H9) of 10 horizons identified for the study area (H1–H10; see legend for color code, which is used for all profiles shown in Fig. 2). In the center of the profile, two near-vertical faults (F) disrupt the sedimentary sequence. Many coral mounds are delineated by a thin black line and some of them show moats. The black box indicates the part of the profile displayed in Table 2. B. Small part of a PARASOUND profile in between the two SWIM faults. This profile shows two still exposed coral mounds, which display recurring phases of mound aggradation. For example, the southern mound initiated on H7 and re-started aggradation during all following horizons. Note that the width of this mound becomes progressively wider with every new re-start of aggradation. C. Sparker profile north of the Renard Ridge indicating several near-vertical faults with the lowest base horizon (H10) being displayed. D. PARASOUND profile between the two SWIM faults showing clustered and exposed coral mounds (black oval). The eastern part of the profile is intensely faulted, while the western part is not and contains several buried mounds.

unit where Late Miocene to Pliocene sediments were deposited in extensional basins, delineated by small tectonic ridges (Flinch, 1993; Maldonado et al., 1999).

The AMCP lies within the southern part of the Gulf of Cádiz and the studied area stretches from 34°50′N to 35°30′N and 6°30′W to 7°15′W (Fig. 1). Water depths in the AMCP range from 200 m on top of the Al Idrisi mud volcano to over 1000 m at the western edges (Fig. 1). Tectonic and structural features in the AMCP consist of two exposed ridges (Vernadsky and Renard Ridges in the north), two large reactivated strike-slip faults (South West Iberian Margin (SWIM) faults 1 and 2; Zitellini et al., 2009) in the center and south (Fig. 1), and many smaller faults in the subsurface (Fig. 2). Extensional tectonic forces account for these features, which is in contrast to the general compressional setting in the Gulf of Cádiz (Flinch et al., 1996). In the northern part of the AMCP, ten mud volcanoes and diapirs and four small sediment drifts are located near the Renard and Vernadsky Ridges (Fig. 1; Van Rensbergen et al., 2005a,b; Vandorpe et al., 2016), while south of the SWIM fault 2, the Meknes mud volcano is present (Fig. 1; Alaoui Mhammedi et al., 2008). Through the deflection of bottom currents, the steepness of the ridges and mud volcanoes greatly influences the location of the sediment drifts (Vandorpe et al., 2016), which provided a first tentative stratigraphic framework for the El Arraiche area. The base of the Quaternary could be determined based on correlation with the nearby LAR-A1 well and is coeval with the onset of mud volcano activity (Van Rensbergen et al., 2005a, b), while the Early-Middle Pleistocene Transition (EMPT) boundary has been identified based on increased acoustic impedance values of the reflectors and is coeval with the cessation of tectonic activity in the region (Vandorpe et al., 2014; Vandorpe et al., 2016). Long-term sedimentation rates in the El Arraiche sediment drift area range between 8 cm kyr^{-1} (during Marine Isotope Stage (MIS) 2 and the Holocene) and 25 cm kyr^{-1} (during MIS 3 and the last deglacial) (Van Rooij et al., 2011; Vandorpe et al., 2014; Wienberg et al., 2010). Recently, Delivet (2017) reported sedimentation rates as high as 100 cm kyr^{-1} during MIS 3 in the Pen Duick drift (core MD08-3227; Fig. 1) and the occurrence of a hiatus of 14 kyr (between 33 kyr and 19 kyr), implying that sedimentation in the sediment drifts was not continuous. Consequently, more erosional events may be present and sedimentation rates could have been even higher at times in the drift systems.

The oceanography of the southern Gulf of Cádiz comprises five distinct water masses: North Atlantic Surface Water between 0 and 200 m, North Atlantic Central Water (NACW) between 200 m and 600 m, Antarctic Intermediate Water (AAIW) between 600 m and 1500 m, Mediterranean Outflow Water occurring as meddies at depths averaging 1000 m and North Atlantic Deep Water below 1500 m (Ambar et al., 2008; Louarn and Morin, 2011; Machín et al., 2006). At the boundary between NACW and AAIW, east-west oriented internal waves are generated, reaching speeds exceeding 30 cm s^{-1} (Mienis et al., 2012; Vandorpe et al., 2016). Little is known about glacial water mass distribution and glacial ocean dynamics in the southern Gulf of Cádiz so far. Two intermediate water masses are reported from this region, being glacial AAIW and glacial North Atlantic Intermediate Waters, located beneath a glacial NACW water mass (Delivet, 2017). Glacial north Atlantic intermediate waters are known to occur down till depths of 2200 m (Marchitto and Broecker, 2006) and may have influenced the AMCP. However, the presence of glacial AAIW, of which the production is known to increase during colder periods (Jung et al., 2011; Wainer et al., 2012), is inferred in the AMCP during colder periods (Vandorpe et al., 2014). Additionally, Delivet (2017) reported more energetic bottom currents during Dansgaard-Oeschger stadials and Heinrich events and even erosive conditions at the foot of the Renard ridge during the Last Glacial Maximum. The causal mechanisms might be related to an increased advection of glacial AAIW, increased salinity of glacial NACW and/or increased pycnal gradients at the glacial NACW/AAIW boundary, leading to higher along-slope velocities and more vigorous internal tidal motions (Delivet, 2017).

3. Material and methods

Two datasets have been combined to investigate the buried coral mounds in the AMCP. The first dataset was obtained in 2013 during the "COMIC" expedition on board of the R/V Belgica and consists of single channel reflection seismic sparker profiles (Figs. 1, 2) comprising 85 profiles covering nearly 650 km in total length (1 m vertical resolution). The energies used were 500 or 600 J, with a shooting rate of 1 or 2 s, depending on the water depth. The data were recorded with a 10 kHz sampling rate and a record length of 0.9 or 1.8 s, again depending on the water depth. Survey speeds were maintained at 3–4 knots. The profiles were processed in order to improve signal-to-noise ratios using the DECO RadexPro software. An Ormsby bandpass filter (75/150 Hz as low-cut ramp and 1250/1500 Hz as high-cut ramp), a swell filter, burst noise removal and spherical divergence corrections were applied.

The second dataset was collected in 2014 during the MSM36 "MoccoMeBo" campaign on board of R/V Maria S. Merian and consists of about 1430 km sub-bottom profiles (SBP ATLAS PARASOUND type P70; decimeter-scale vertical resolution; Figs. 1, 2). The maximum transmission power was 70 kW with a maximum penetration of 200 m. The beam width of the primary (19.3 kHz) and secondary (3.85 kHz) frequencies was 4° by 4.5° and 4° by 5°, respectively. Maximum transmission voltage was set at 100–120 V and the receiver amplification at 15 dB. Survey speeds were kept at 2 to 4 knots. The sub-bottom profiles were recorded with ATLAS PARASTORE software and processed in several steps. The first step includes the transition from the *.ps3 format into the *.segy format using the ps32segy software of Dr. Hanno Keil (University Bremen). The second step was performed using the REFLEXw software (vers. 7.2.2) and consisted of a static correction, muting of the water column and applying an automatic gain control. The final processing step was performed with the DECO RadexPro software and consisted of calculating a Hilbert transform, removing burst noise and applying a spherical divergence correction.

For all coral mounds, the base horizon was mapped and correlated throughout the AMCP along the SBP and seismic profiles. Several parameters were defined for each coral mound: coordinates, width (at several cross-sections), height and the depth of the seafloor above the coral mound. The total mound volume (TMV) for each mound was calculated assuming an ideal demi-ovoid shape by using the following formula:

$$TMV = \frac{\pi^* height^* \left(\frac{width_{max}}{2}\right)^2}{3}$$

Due to the 2D nature of the seismic methods, the measured widths, heights and calculated TMV's of the coral mounds have to be considered as their minimum dimensions as the mounds might have a far more complex shape, not represented by the 2D crosscut. As a consequence, the mound dimensions given in this paper have to be interpreted with caution, bearing in mind that the true dimensions may be deviant. The depth of the seafloor and the height of the mound were transferred from seconds two-way-travel time (TWT) to meters using seismic

Table 1
Overview of the root mean square and interval velocities used to convert the heights (seconds two-way-travel time) of the coral mounds into meters based on an amplitude versus offset experiment (Van Rooij et al., 2005; location, see Fig. 1). The left column indicates the depth below seafloor of the upper boundary of the interval.

$T_{subsurface}$ (ms TWT)	RMS velocity (m/s)	Interval-velocity (m/s)
0	1502.142	1502.142
99.1	1513.331	1609.995
215.1	1547.495	1829.109
354	1599.937	2004.367
434.4	1637.555	2204.469
749.4	1792.402	2426.758

velocities determined by a wide angle test in 2005 (location indicated as AVO in Fig. 1; resulting velocities indicated in Table 1; AVO test discussed in Appendix A.1).

From the heights and TMV's of the mounds rooting on each horizon, a histogram was constructed and the probability distribution was modelled with a log-logistic function (e.g. for the height of mounds rooting on H3 displayed in Fig. 3A, B). The correlation coefficient between histogram and fit was always high (around 0.99). From the log-logistic fit, the 5% percentile, mode and 95% percentile of the height and TMV were calculated and plotted for each horizon (Fig. 3C, D).

4. Results

By analyzing the seismic and sub-bottom (PARASOUND) data, a total of 781 coral mounds were identified for the AMCP (Table 2). From these 781 coral mounds, 615 are fully buried by sediments, while 166 are still exposed and arise several meters above the seafloor (Fig. 2A, B, D). However, considering the limitation in penetration of the PARASOUND sub-bottom profiler (mostly <80 m, Fig. 2) and the areal coverage of the surveyed areas (limited to profile lines), the ultimate number of exposed as well as buried mounds is likely considerably higher.

4.1. Seismic characteristics

Both in the reflection seismic and sub-bottom (PARASOUND) datasets, buried mounds can be recognized due to their (almost) acoustically transparent facies (Fig. 2). Small coral mounds (up to 20 ms TWT) appear mostly as transparent structures embedded within well-stratified sub-horizontal reflectors (Fig. 2A, C, D), while larger coral mounds (>20 ms TWT; Fig. 2B) may contain small chaotic reflections and diffraction hyperbola. The mounds may affect the surrounding sediments as small moat-like structures are sometimes present (Fig. 2) or as the overlying sediments have a mounded appearance once mound aggradation

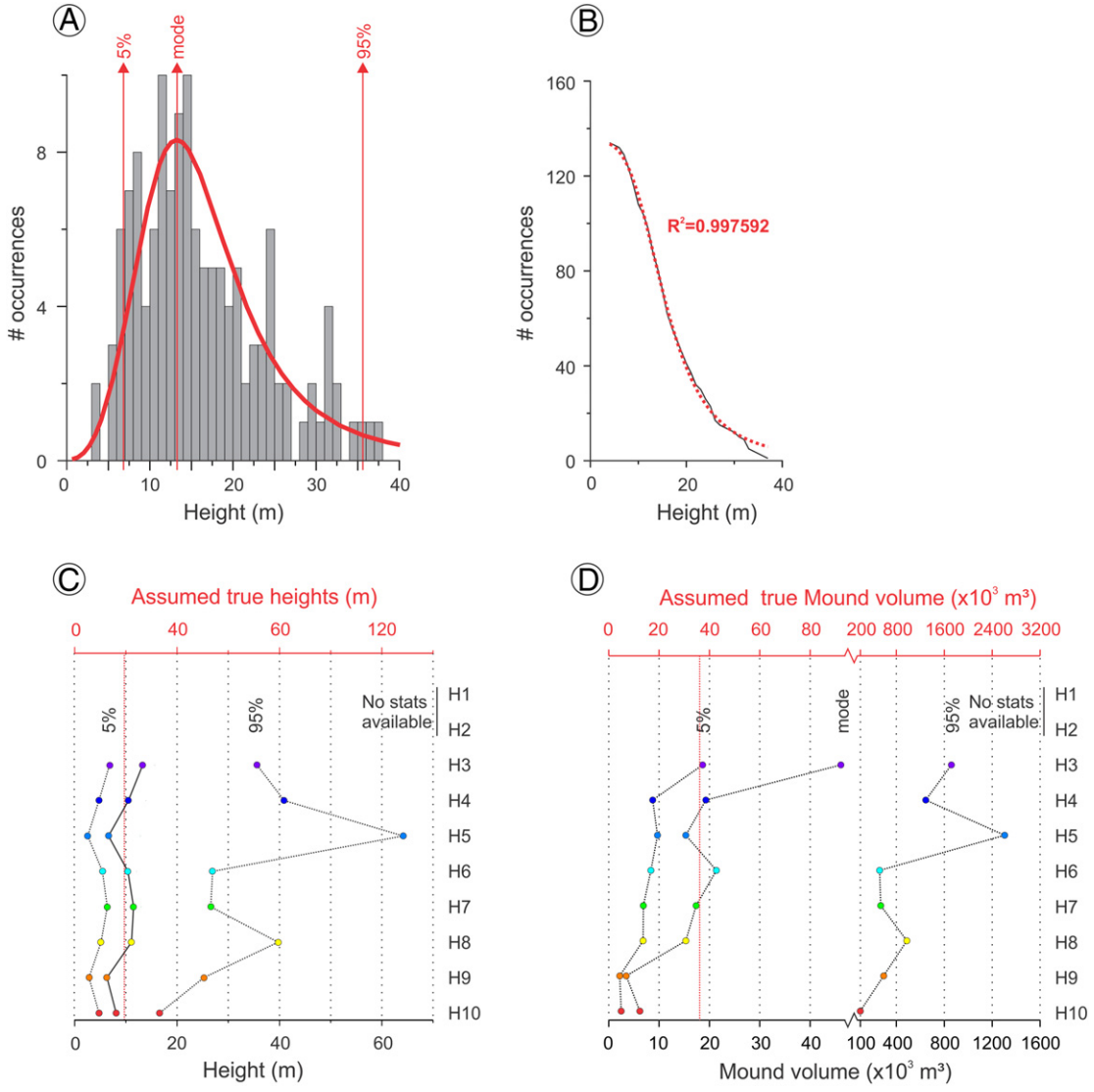

Fig. 3. A. Histogram of the height of the mounds rooting on horizon 3 with indication of the log-logistic fit (red). B. Cumulative distribution of the height of the mounds of horizon 3 (black) and log-logistic fit (red). C. Evolution of the height of the mounds rooting on the different horizons based on the log-logistic fit. For the upper two horizons H1 and H2, no statistical information is calculated due to the low number of identified mounds for these horizons (respectively 6 and 16; Table 2). The red striped line indicates the average of the modes of the 10 horizons. The red axis on top of the plot is twice the actual measured heights and displays the assumed true average heights of the coral mounds for each horizon. D. Evolution of the TMV (total mound volume) of the mounds rooting on the different horizons based on the log-logistic fit. For the upper two horizons H1 and H2, no statistical information is calculated due to the low number of identified mounds for these horizons (respectively 6 and 16; Table 2). The red striped line indicates the average of the modes of the 10 horizons. The red axis on top of the plot is twice the actual measured TMV's and displays the assumed true average TMV's of the coral mounds for each horizon.

Table 2
Statistical evaluation of coral mounds in the AMCP. Column 1: Seismic expression of 9 of the 10 horizons based on the PARASOUND profile of Fig. 2A. Column 2: Number of horizons identified to act as a base for mound formation. Columns 3/4: Amount and percentage of mounds rooting on each of the 10 horizons. Columns 5/6: Amount and percentage of coral mounds still having an exposed position at the seabed surface in relation to the 10 horizons. Column 7: The average water depth where the coral mounds occur.

Seismic expression	Horizon	Mounds		Exposed		Average depth
		Amount	Percentage	Amount	Percentage	(m)
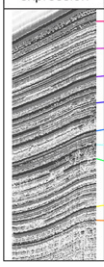	1	6	0.8%	3	50.0%	716.8
	2	16	2.0%	14	87.5%	808.7
	3	135	17.3%	93	68.9%	882.7
	4	119	15.2%	37	31.1%	849.4
	5	40	5.1%	13	32.5%	834.0
	6	124	15.9%	2	1.6%	740.0
	7	66	8.5%	2	3.0%	814.4
	8	143	18.3%	2	1.4%	725.7
	9	62	7.9%	0	0%	731.4
	10	70	9.0%	0	0%	701.4

has ceased (Figs. 2A, B & D). Within the sedimentary sequence (which can be up to 400 ms TWT), many faults are observed (Fig. 2A, C, D). Offsets are mostly only a few ms TWT (Fig. 2A, D), but some faults have offsets >10 ms TWT (Fig. 2C).

4.2. Horizon description

Ten horizons (H10 — H1) were identified in the sedimentary sequence of the AMCP, on which the Moroccan coral mounds have

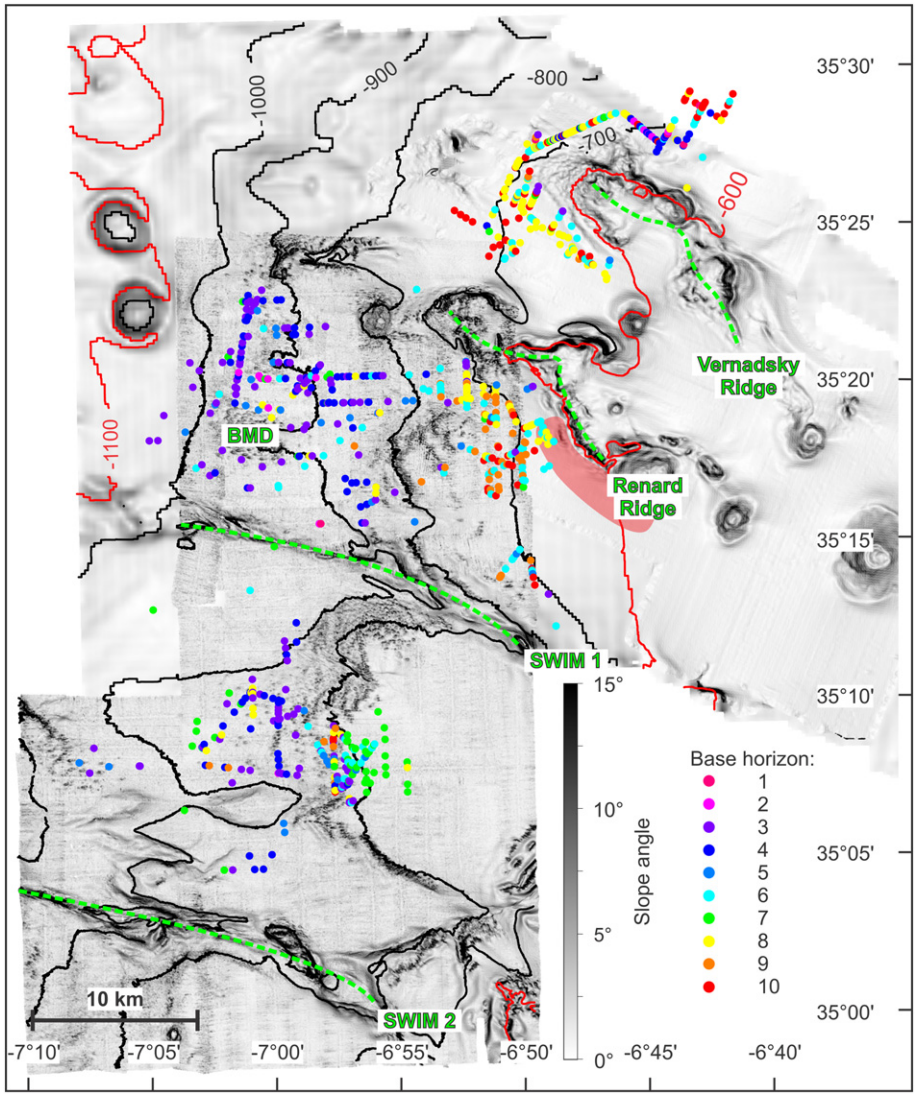

Fig. 4. The position of the identified coral mounds (color-coded based on their base horizon, see legend) with a map of the slope angle as a background (grey scales). The 600 m and 1100 m contour lines are indicated in red. The green dashed lines indicate (from north to south) the Vernadsky Ridge, the Renard Ridge, SWIM fault 1 and SWIM fault 2. The red area indicates the extent of the Pen Duick drift. BMD: Becks mud diapir, SWIM: Southwestern Iberian Margin.

initiated in the past (regardless if they are fully buried or are still exposed at the seafloor). These horizons were numbered from top to bottom (Figs. 2, 3).

Horizon 10 is the top reflector of a package of moderate to high amplitude reflectors (Fig. 2C). On top of this horizon, a package of low-amplitude reflectors with intermittent high amplitude reflectors is present. Due to the limited penetration of the PARASOUND signal, H10 can only be observed on the sparker profiles. Coral mounds initiating on H10 (in total 70) were mainly identified close to the 700 m bathymetric contour line around the Vernadsky Ridge and south of the Renard Ridge. Five mounds rooting on H10 were also identified between the two SWIM faults (Fig. 4).

Horizon 9 is the lower of two strong reflectors within a sequence of mostly low-amplitude reflectors (Fig. 2C). It was mainly indicated by the sparker data, while it is only visible on some of the PARASOUND profiles. The 62 coral mounds initiating on H9 mostly occur directly south of the Renard Ridge (84%) with occurrences around the Vernadsky Ridge (5) and between the SWIM faults (6) as well (Table 2; Fig. 4).

Horizon 8 is recognized as a strong reflector when not positioned too deep (up to 100 ms TWT below the seafloor; Figs. 2B, D) but is far less pronounced when more sediments have been deposited on top (150–200 ms TWT; Fig. 2C). A total of 143 coral mounds (~18% of all identified mounds in the AMCP; Table 2) were observed to initiate on H8. This is the largest number of mounds identified for any of the ten horizons. The majority of H8-mounds (~85%) occur directly around the Vernadsky Ridge and south of the Renard Ridge, while just ten mounds were identified around the Becks mud diapir in the westernmost part of the AMCP and 14 mounds are positioned between the SWIM faults (Table 2; Fig. 4).

Horizon 7 is identified as a higher-amplitude base reflector in a small package of low-amplitude reflections. This low-amplitude package is positioned between two higher-amplitude packages (Figs. 2A, B, C). The majority (61%) of the 66 identified coral mounds originating on H7 are found clustered in a small area between the two SWIM faults confined to a water depth of 800 m, while others are scattered over the entire AMCP (Fig. 4).

Horizon 6 is recognized on the profiles as the lower boundary of a high amplitude interval of several reflectors, with the upper boundary of this interval being marked by H5 (Figs. 2A, B). A total of 124 coral mounds (~16% of all identified mounds in the AMCP; Table 2) that initiated on H6 occur mostly (about 87%) north of the SWIM fault 1 and 16 mounds are also observed between both SWIM faults (Fig. 4). In contrast to H6, a rather low number of coral mounds ($n = 40$; ~5% of all identified mounds in the AMCP; Table 2) initiated on H5, whereby 27 mounds occur between the SWIM fault 1 and the Renard Ridge, while 13 mounds are present south of the SWIM fault 1 (Fig. 4).

Horizon 4 is characterized by a very low amplitude reflector (Fig. 2). Coral mounds ($n = 119$; Table 2) rooting on this horizon occur everywhere in the AMCP. South of the Vernadsky Ridge, H4-mounds are confined to a water depth interval between 800 m and 1000 m, while those directly surrounding the Vernadsky Ridge occur at 650 m water depth (Fig. 4).

Horizon 3 is the reflector with the highest amplitudes present in the sedimentary sequence in the AMCP (Fig. 2; Table 2). It can be recognized throughout the area and 135 coral mounds (~17% of all identified mounds in the AMCP; Table 2) initiate on this horizon. The mounds rooting on H3 occur mainly in an 8 km radius around the Becks mud diapir and in a cluster between the SWIM faults (~65%), corresponding to a water depth interval of 800 m to 900 m (Fig. 4).

Horizon 2 is recognized in the sedimentary deposits as the top of a high amplitude interval (Figs. 2A, C), while H1 is a high-amplitude reflector, which occurs only a few ms TWT below the seafloor. The sixteen coral mounds that were identified to have initiated on H2 (2% of all identified mounds in the AMCP; Table 2) are all but one positioned north of the SWIM fault 1, while five of a total of six mounds identified for H1 (<1% of all identified mounds; Table 2) occur around the Vernadsky Ridge (Fig. 4). A lot of mounds, from which the base horizon cannot be determined, are present on the steep slopes of the AMCP (Fig. 2D). As a consequence, more mounds, rooting on several (possibly until now undiscerned) horizons are expected to be present in the AMCP.

4.3. Coral mound characteristics

Due to the limited number of coral mounds rooting on H1 ($n = 6$) and H2 ($n = 16$), contributing to <3% of all identified mounds in the AMCP (Table 2), they are not considered for the statistical analyses (Fig. 3C, D). All other horizons show a high number of mounds rooting on them, ranging from 40 mounds identified for H5 to 143 mounds for H8 (Table 2).

All coral mounds in the AMCP are found within a water depth range of 600 m to 1100 m (marked by red lines in Fig. 4). Based on the averaged present-day water depths for all coral mounds rooting on one horizon, a trend towards an increasingly deeper location is observed going from H10 (701.4 m) to H3 (882.7 m), with a large exception for H6 (740 m) (Table 2).

Some of the larger coral mounds towered a fair amount above the palaeo-seafloor, still exhibiting a positive topography when the next initiation phase occurred, after which they were re-colonized, seemingly displaying continuous coral mound growth (e.g. several H4-mounds in the eastern part of Fig. 2A or the mounds displayed in Fig. 2B). At present, 166 coral mounds still surface on the seafloor, none of which root on the deepest horizons H10 and H9. For the following three horizons (H8-H6) only 2 mounds of each horizon (1.4–3% of the total number of mounds identified per horizon) still pierce the seafloor (Table 2). From H5 onwards, the percentage of exposed mounds contributing to the total number of mounds strongly increases to over 30% as identified for H5 and H4, and to even ~70% of mounds rooting on H3 (Table 2). As the base horizon for many exposed mounds is not easy to discern, the percentage of exposed mounds rooting on H2 and H1 will likely even be higher than 70%.

The 5th percentile (indicating the average height of the smaller mounds) together with the mode of the heights show a continuous trend with similar values for H8, H7, H6 and H4 (between 4.7 m and 6.4 m and between 10.5 m and 11.4 m respectively) and lower values for H10, H9 and H5 (between 2.6 m and 4.8 m and between 6.3 m and 8.1 m respectively). Horizon 3 has the highest height-values for these parameters compared to all other horizons (6.8 m and 13.3 respectively). The 95th percentile for the heights (indicating the average height of the tallest mounds) varies differently and no clear trend is observed. H5 reveals much larger values (64.1 m) compared to the other horizons. The 5th percentile and mode of the TMV for horizons H8, H7, H6, H5 and H4 are similar (between 6.8×10^3 m^3 and 8.7×10^3 m^3 and between 15.3×10^3 m^3 and 21.4×10^3 m^3 respectively), while lower values for H10 and H9 (between 2.2×10^3 m^3 and 2.5×10^3 m^3 and between 3.5×10^3 m^3 and 6.2×10^3 m^3 respectively) are observed (Fig. 3D). The 95th percentile of the TMV and height display a similar trend, with values for the TMV ranging between 98.8×10^3 m^3 and 1304.2×10^3 m^3 (Fig. 3C). The large variation of the 95th percentile of both height and TMV may be caused by the skewed distribution of the heights and TMV's towards smaller mounds (e.g. Fig. 3A).

The height of the coral mounds being deduced from the seismic lines has to be interpreted with caution as these lines only represent a 2D slice of a 3D volume. However, when a large number of mounds is measured, the obtained average height will be close to 50% of the real average height. As a result, an actual average height twice the obtained average height (red axis in Fig. 3C) and an actual average TMV twice the actual TMV (red axis in Fig. 3D) can be assumed. Consequently, relative changes between average heights and TMV's measured for mounds rooting on the individual horizons might be discussed.

5. Discussion

A large amount of acoustically transparent features is present within both geophysical datasets (Fig. 2), which have been interpreted as coral mounds considering the striking similarities (both in acoustic appearance and morphology) with buried coral mounds in the Porcupine Seabight (Huvenne et al., 2007; Pirlet et al., 2010). Transparent features can also indicate pockets of gas, fluid flow features or mass wasting of sediments (e.g. turbidites or mud extrusions). However, these origins can be excluded for the transparent features identified for the AMCP. For instance, mass wasting deposits are usually laterally continuous and have much larger dimensions (up to tens of kilometers long, e.g. Haines et al., 2017 and Moernaut et al., 2010), while mud extrusions are confined to the vicinity of the mud volcanoes themselves. Pockets of gas and fluid-flow features usually do not have a well-delineated cone or ovoid shape, are rather shapeless and blurred (Haines et al., 2017; Plassen and Vorren, 2003) or create acoustic chimneys (Somoza et al., 2014). Neither of these characteristics apply to the features observed in the AMCP (Fig. 2). Additionally, some of the numerous exposed coral mounds being present in the AMCP root on the same reflectors as the buried mounds. These exposed mounds have been drilled with the seafloor drill rig MeBo70 during the MoccoMeBo campaign (MSM36) in 2014. Up to 30 m long coral-bearing sediment cores were recovered, some even penetrating the base of the mounds, ultimately proving their true coral mound nature (Hebbeln et al., 2015).

5.1. Temporal variability of coral mound occurrence

Regarding the Atlantic coral mound realm, there are just a few areas known for which buried coral mounds were identified so far. One of the best studied areas is the Porcupine Seabight along the Irish margin, where buried mounds were found within the Magellan mound province (De Mol et al., 2002; Huvenne et al., 2003; Huvenne et al., 2007), and seem to have been originated on one single reflector (Huvenne et al., 2007; Huvenne et al., 2009). For the SW Rockall Trough, three potential/possible horizons for mound initiation were reported (van Weering et al., 2003) and in the westernmost part of the Mediterranean Sea (Alboran Sea) also three initiation horizons could be distinguished (Lo Iacono et al., 2014).

In contrast, for the AMCP, at least ten initiation events comprising distinct generations of coral mounds were identified, with several mounds restarting aggradation at one of the following horizons (Fig. 2). Within the southern H7 coral mound of Fig. 2B, a small package of reflectors is present within the mound immediately below H3, indicating that mound aggradation had ceased for a while between H4 and H3. However, from H3 onward, mound aggradation restarted at that location with the coral mound still piercing the present-day seafloor. This indicates that some of the buried coral mounds experienced several recurring periods of CWC colonization and coral framework growth resulting in pronounced mound aggradation followed by coral demise and subsequent stagnation in mound aggradation or even mound erosion. This pattern in mound development alternating between active and dormant mound phases has already been described for several other coral mound areas in the North Atlantic (e.g. Kano et al., 2007; Eisele et al., 2011; López Correa et al., 2012; Matos et al., 2015). Since no absolute (coral) ages have been obtained from the Moroccan buried mounds so far, a correlation with the Quaternary Pen Duick drift was conducted (Vandorpe et al., 2014; Fig. 5). The most pronounced seismic stratigraphic change in this drift system is the transition from sheeted to mounded drift deposits since the EMPT (red line in Fig. 5), which is expressed by increasing reflection amplitudes (Vandorpe et al., 2014) and the accompanied cessation of tectonic activity. This boundary is coeval with H10, pointing to a post-EMPT period in coral mound aggradation in the AMCP. Following this correlation, average sedimentation rates in the Renard drift (Fig. 1) would be 20.1 cm kyr^{-1} (using the depths along the line in Fig. 2C and the interval-velocities of Table 1). This rate is within the range of reported sedimentation rates varying between 8 and 25 cm kyr^{-1} (Van Rooij et al., 2011; Vandorpe et al., 2014; Wienberg et al., 2010).

Coral ages obtained from this region show that 75% of all ages coincide with glacial periods (going back to MIS 12; Fig. 6), implying that both the occurrence of CWC and coral mound aggradation are mostly restricted to cold periods in the AMCP (Frank et al., 2011; Wienberg et al., 2009; Wienberg et al., 2010). Given (1) the climate-related periodic on- and off-set in coral mound aggradation documented for coral mound areas all over the Atlantic Ocean (Frank et al., 2011), (2) the fact that ten horizons (being the base for Moroccan mound initiation) were discerned from the EMPT onwards, and that (3) the reported

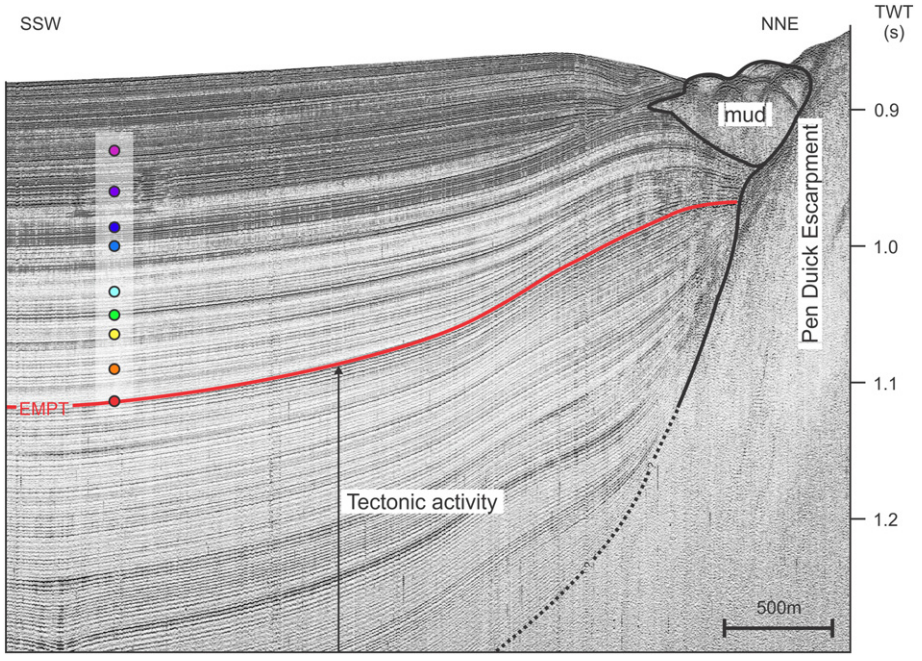

Fig. 5. Correlation between the Pen Duick drift (Vandorpe et al., 2014) and 9 of the 10 identified horizons. H1 could not be correlated to this profile. EMPT: Early-Middle Pleistocene Transition TWT: Two-Way Travel Time.

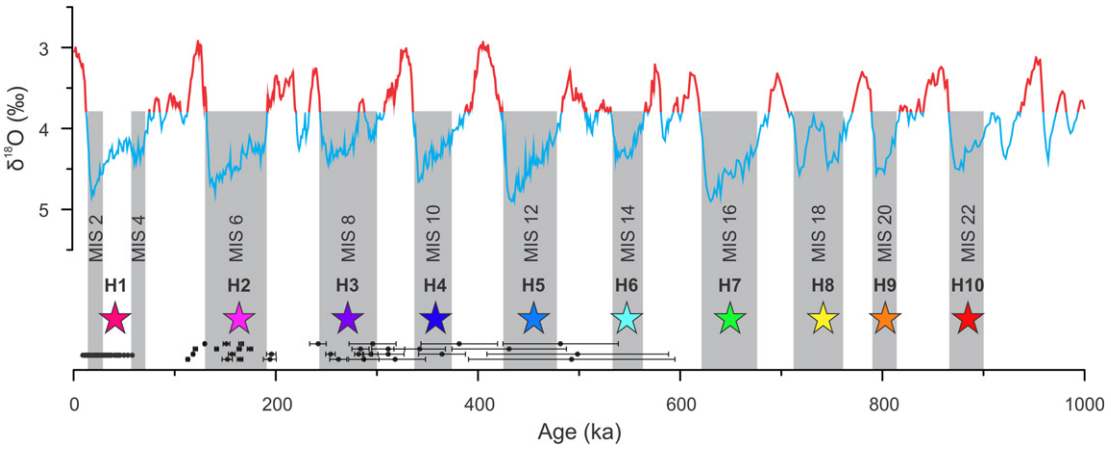

Fig. 6. Tentative correlation between the ten horizons (stars) acting as a base for the initiation of coral mounds and the Marine Isotopic Stages (MIS; boundaries between MIS are based on the stable oxygen isotope LR04 stack by Lisiecki and Raymo (2005)). The black dots indicate cold-water coral ages obtained from the mound-forming species *Lophelia pertusa* and *Madrepora oculata* collected from various exposed mounds in the AMCP (Frank et al., 2011; Wienberg et al., 2009; Wienberg et al., 2010).

coral ages show that colder (glacial) periods offered more suitable environmental conditions triggering the sustained occurrence of CWC and thus the aggradation of coral mounds in the AMCP (at least during the past ~500 kyr) (Frank et al., 2011; Wienberg et al., 2009; Wienberg et al., 2010), the ten identified initiation events (horizons) might be assigned to cold (glacial) periods occurring since the EMPT (Lisiecki and Raymo, 2005). As such, a preliminary chronostratigraphy, displayed in Fig. 6, is obtained and may serve as a first approximation of coral mound aggradation periods in the AMCP, although dating will be required to finally verify this. As discerning the base horizon of many mounds on the steeper parts of the AMCP was not possible (e.g. Fig. 2D), more horizons may be present and more than one initiation event may have occurred in the course of one glacial cycle.

The three horizons with the highest acoustic amplitudes (H3, H6 and H8; Fig. 2, Table 2) also represent the initiation base for >50% of all coral mounds identified in the AMCP (Table 2). High amplitude values are usually caused by a facies change, such as a change from fine-grained (silty) to coarse-grained (sandy) sediments, inducing a difference in acoustic impedance. Indeed, two long (up to 45 m) off-mound MeBo cores recovered in the AMCP revealed overall silty sediments down to a drill depth of 30 m, while below several centi- to decimeter thick layers composed of well-sorted, dark fine sands are intercalated (Hebbeln et al., 2015). These layers might correspond to one of the horizons with higher acoustic amplitudes and may either be derived from contouritic or turbiditic processes. Three main factors contradict a turbiditic origin for these horizons. Firstly, the three horizons (especially H3 and H8) can be observed margin-wide, which is not consistent with turbidite deposits on continental slopes, which are expected to be focussed in channels or levees (Picot et al., 2016; Piper and Normark, 2009; Stow and Mayall, 2000). Secondly, the fairly low slope angle of the margin (usually below 1°; Fig. 4) in combination with the low average sedimentation rates (Delivet, 2017; Wienberg et al., 2010) are not in favour of slope failure that could cause turbidite deposits (Piper and Normark, 2009). And thirdly, the dark fine sands in the lower parts of two off-mound MeBo-cores are well-sorted (Hebbeln et al., 2015), which is not consistent with turbidite deposits. Contourites and the bottom currents associated with them on the other hand are known to occur widespread in this region (Vandorpe et al., 2016). Although the depositional and erosional features of these bottom currents are largely restricted to the areas bordering the main topographic features in the AMCP such as the Pen Duick escarpment (Vandorpe et al., 2016), bottom currents usually do create regionally rather widespread (erosional) horizons. Given the occurrence of >50% of the identified coral mounds on the highest acoustic amplitude layers and the likely bottom current-controlled origin of these layers, the number of coral mounds that initiate in a certain period may be controlled by the intensity of the bottom currents. Since bottom currents and the AAIW, present within the depth ranges of the coral mounds of the AMCP (600 m to 1100 m; Fig. 1; Vandorpe et al., 2016), themselves are known to be strongly influenced by climate (Jung et al., 2011; Makou et al., 2010; Rebesco et al., 2014), the base horizons (and hence mound initiation) may be strongly climate-controlled as well.

5.2. Coral mound dimensions and location

The AMCP is one of the largest coral mound provinces discovered so far in the world, covering an area of over 1800 km^2, consisting of at least 615 buried coral mounds and 166 exposed coral mounds. In comparison, the Campeche coral mound province in the southern Gulf of Mexico (>40 km^2; Hebbeln et al., 2014), the Røst Reef (>120 km^2) and the Traena Reefs (about 300 km^2) along the Norwegian margin (Fosså et al., 2005) and the Magellan (about 1200 km^2) and Hovland (about 380 km^2; Huvenne et al., 2003) coral mound provinces in the Porcupine Seabight are all considerably smaller. When comparing the density of buried coral mounds in the Magellan mound province (0.93 mounds km^{-2}; Huvenne et al., 2003) to that of the AMCP (0.43 mounds km^{-2}), it is noticed that while the AMCP covers a much larger area (by a factor of 15), the density of coral mounds in this area is not considerably smaller (by a factor of 2.1). The average height of the coral mounds in the AMCP (defined here as the average of the modes of the 10 horizons) is about 20 m (red line in Fig. 3C) and is among the smallest observed in the North Atlantic, in particular when compared to coral mounds of the Magellan, Hovland and Belgica mound provinces of the Porcupine Seabight with average mound heights varying between 70 m and 100 m (De Mol et al., 2002; Huvenne et al., 2007) or to coral mounds along the Mauritanian margin with an average height of 100 m (Colman et al., 2005). The average TMV of the coral mounds in the AMCP (defined here as the average of the modes of the 10 horizons) is 36.1 $\times 10^3$ m^3 (Fig. 3D) and is 34 times smaller compared to the average TMV of coral mounds from the Magellan mound province (1200 $\times 10^3$ m^3, derived by applying the same formula described above to the dimensions given by Huvenne et al. (2003)). Also compared to the West-Melilla coral mounds in the western Mediterranean Sea, which are between 227 and 1060 $\times 10^3$ m^3 (Lo Iacono et al., 2014), the AMCP coral mounds have a 6–30 times smaller TMV.

The overall very low TMV (up to 34 times smaller) and mound heights (up to 5 times smaller) of the Moroccan buried mounds point to rather low aggradation rates. This is already indicated for the exposed mounds in the area, for which glacial mound aggradation rates of 1–53 cm kyr^{-1} are calculated (Wienberg and Titschack, 2017), being in the lower range of rates compared to the Irish and Norwegian coral

mounds (up to 220 cm kyr^{-1} and 1500 cm kyr^{-1} respectively; Frank et al., 2009; Titschack et al., 2015). Mound aggradation is controlled by sustained CWC growth and a contemporary input of sediments, which are baffled by the open coral framework, stabilizing the biogenic framework and allowing continued, enhanced vertical aggradation (e.g. Hebbeln et al., 2016; Huvenne et al., 2009; Titschack et al., 2015; Wienberg and Titschack, 2017). Average sedimentation rates between 10 and 25 cm kyr^{-1} have been reported from the AMCP drift systems (Van Rooij et al., 2010; Vandorpe et al., 2014; Wienberg et al., 2010), although erosional features and higher sedimentation rates of up to 100 cm kyr^{-1} were inferred by Delivet (2017) in the Pen Duick drift during MIS 3 (core MD08-3227; Fig. 1). However, outside the El Arraiche drift systems (Vandorpe et al., 2016), where most of the coral mounds are situated (Figs. 1, 4), average sedimentation rates are as low as ~2 cm kyr^{-1} (Delivet, 2017), indicating an overall sediment-starved margin. In comparison, the Irish coral mounds of the Porcupine Seabight and the Rockall Trough, whose formation was restricted to the recent Holocene and previous interglacial periods (e.g. Frank et al., 2011; Kano et al., 2007; Mienis et al., 2009), correspond to sedimentation rates of up to 25 cm kyr^{-1} and around 10 cm kyr^{-1} respectively (Mienis et al., 2009; Rüggeberg et al., 2007; Van der Land et al., 2010; Van Rooij et al., 2007). Thus, the rather low sedimentation rates indicated in the AMCP possibly explain the small dimensions of the Moroccan coral mounds. Even though sediment availability was limited to maintain coral mound aggradation, increased bottom currents (leading to hiatuses in the Pen Duick drift; Delivet, 2017) during glacial periods may have flushed sufficient sediment particles through the coral framework, allowing them to baffle enough sediment for coral mound aggradation (Hebbeln et al., 2016) and the build-up of small coral mounds. Similar conditions have already been reported from the Porcupine Basin, where coral mounds were built up under erosive conditions (Dorschel et al., 2009). The higher average TMV and height of mounds rooting on H3 (92.2×10^3 m^3 and 26.6 m respectively; Fig. 3C and D) may result from a temporary higher baffling capacity of the CWC framework or from the availability of more sediments during MIS 3 (Fig. 6). A mechanism indicated by Glogowski et al. (2015) for the southern Moroccan mounds as well.

5.3. Lateral variability and clustering of coral mound occurrence

The optimal conditions for coral mound initiation may have progressively moved towards deeper areas as the average depth for the successive horizons changes from 701.4 m for H10 to 882.7 m for H3 with the exception of H7 where the average depth is 814.4 m (Table 2). The largest change occurs at H5, where water depths increase rather abruptly from ~700–740 m (H10–H6) to ~830–880 m water depth (H5–H3). As most of the coral mounds rooting on H4 and H3 cluster around the Becks mud diapir or between the two SWIM faults (Fig. 4), the optimal conditions for CWC growth and thus mound aggradation must have shifted to those deeper regions.

Clusters of buried coral mounds have been discerned in the AMCP (Fig. 4), with all of them containing coral mounds from several horizons. Clustering of mounds is not only observed in the AMCP, but occurs in many mound provinces, e.g. in the Porcupine Seabight (De Mol et al., 2002), the Gulf of Mexico (Hebbeln et al., 2014) or off the southern Atlantic Moroccan coast (Glogowski et al., 2015). The small coral mounds can deflect bottom currents, which is evidenced by the presence of small moats around some of the buried coral mounds (Fig. 2A), similar to the small-scale contourites around the Campeche coral mounds (Hebbeln et al., 2012). Deflection of bottom currents will enhance the current speeds (Rebesco et al., 2014) and may bring more food particles and sediments to the neighbouring coral mounds (Hebbeln et al., 2016). As coral mounds in many cases cut through the subsequent base horizon (Fig. 2), indicating they had an exposed position when the next initiation phase occurred, they could create a locally more favorable environment, leading to continued coral growth in that cluster. This is evidenced by the presence of several horizons in one cluster (Fig. 4). Moreover, besides continued coral growth in that particular cluster, the coral mound will be exposed to accelerated bottom currents (Wienberg and Titschack, 2017), making recolonization of the coral mound by CWC and renewed coral mound aggradation more likely.

6. Conclusions

With an extension of 1800 km^2, the AMCP along the Atlantic Moroccan margin is one of the largest coral mound provinces worldwide discovered so far. Moreover, this mound province is unique in the Atlantic realm as hundreds of exposed as well as fully buried coral mounds exist in this area, which represent different generations of coral mounds as they initiated on at least ten horizons, while for most other Atlantic mound provinces, only one single rooting horizon was indicated. The ten horizons in the AMCP could all be tentatively traced back to glacial periods since the Early-Middle Pleistocene Transition, meaning that favorable conditions for mound initiation and subsequent aggradation occurred several times during the last 900 kyr along the Atlantic Moroccan margin. As a consequence, a strong climatic control on mound initiation and aggradation can be inferred in this region.

The relatively small heights and volumes of coral mounds (~20 m and 36.1×10^3 m^3) in this region might indicate that a reduced/restricted/relatively low sediment input may have prevented the development of giant mounds as found along the Irish margin. Recolonization by CWC and renewed mound aggradation was possible when coral mounds were still exposed during the subsequent initiation phase. Clustering can intensify bottom currents locally and improve both food and sediment supply to the coral mounds.

The timing of the mound initiation, mound aggradation and coral demise cannot be determined from seismic data alone and as a consequence, datings of coral fragments from sediment cores penetrating the coral mounds are necessary to further understand the forcing mechanism. The AMCP can play a vital role in further unravelling the factors that trigger coral mound initiation and aggradation due to the ubiquitous presence of small coral mounds rooting on multiple horizons and its unique position close to contourite drifts.

Acknowledgements

This work frames in both the “Contourite 3D” project (no 1.5.247.13N) funded by the Research Foundation - Flanders (FWO) and contributes to the project “MoccAMeBo – Climate-driven initiation and development of cold-water coral mounds along the Moroccan Atlantic margin revealed by MeBo-cores” (grant He 3412/18) funded by the Deutsche Forschungsgemeinschaft (DFG). We thank the officers and crews of the R/V Belgica and the R/V Maria S. Merian as well as the scientific crews for on-board assistance during cruises “COMIC” (R/V Belgica, 2013) and MSM36 “MoccoMeBo” (R/V Maria S. Merian, 2014). Ship time onboard the R/V Belgica was provided by BELSPO and RBINS-OD nature. The MSM36 “MoccoMebo” cruise was further supported by the DFG Research Center/Cluster of Excellence “MARUM – The Ocean in the Earth System”. The metadata used for this study are available through “Pangaea” (PDI-15151). We also acknowledge Veerle Huvenne and one anonymous reviewer for their extremely helpful comments, greatly improving the content of this paper. Finally, we wish to dedicate this paper to the memory of Jean-Pierre Henriet, a pioneer in cold-water coral research.

Appendix A

A.1. Calculation of the interval-velocities based on the AVO (amplitude versus offset) test

The AVO (Amplitude versus Offset) test (Van Rooij et al., 2005) consisted of two vessels (R/V Belgica and R/V Pelagia) approaching a common point (2 km south of the Pen Duick Escarpment, indicated as

AVO in Fig. 1) and receiving the signal of each other sources. The distance between source and receiver (x) was deduced from the direct wave and an assumed average seismic velocity in the water of 1500 ms^{-1}. Besides the seafloor, five other reflectors were picked and the velocity was determined based on the following equation:

$$t^2 = t_0^2 + \frac{x^2}{v^2}$$

t_0 for all six horizons was determined from the signal of the nearest point based on:

$$t_0^2 = t_{\text{receiver}}^2 - t_{\text{direct}}^2$$

The root mean square velocity was calculated based on the mapping of these horizons along the seismic line. Based on the root mean square velocity, the interval velocity could be determined using the following formula:

$$v_{\text{interval}}^2 = \frac{v_{rms}^2{}^{*} t_n - v_{rms}^2 * t_{n-1}}{t_n - t_{n-1}}$$

References

Alaoui Mhammedi, N., El Moumni, B., El Hmaidi, A., Raissouni, A., El Arrim, A., 2008. Mineralogical and geochemical study of mud volcanoes in north Moroccan Atlantic margin. Afr. J. Environ. Sci. Technol. 2, 387–396.

Ambar, I., Serra, N., Neves, F., Ferreira, T., 2008. Observations of the Mediterranean undercurrent and eddies in the Gulf of Cadiz during 2001. J. Mar. Syst. 71, 195–220.

Colman, J.G., Gordon, D.M., Lane, A.P., Forde, M.J., Fitzpatrick, J.J., 2005. Carbonate mounds off Mauritania, Northwest Africa: status of deep-water corals and implications for management of fishing and oil exploration activities. In: Freiwald, A., Roberts, J.M. (Eds.), Cold-water Corals and Ecosystems. Springer, Berlin, Heidelberg, pp. 417–441.

Davies, A.J., Guinotte, J.M., 2011. Global habitat suitability for framework-forming cold-water corals. PLoS One 6, e18483.

Davies, A.J., Wisshak, M., Orr, J.C., Roberts, M.J., 2008. Predicting suitable habitat for the cold-water coral *Lophelia pertusa* (Scleractinia). Deep-Sea Res. I Oceanogr. Res. Pap. 55, 1048–1062.

De Mol, B., Van Rensbergen, P., Pillen, S., Van Herreweghe, K., Van Rooij, D., McDonnell, A., Huvenne, V., Ivanov, M., Swennen, R., Henriet, J.P., 2002. Large deep-water coral banks in the Porcupine Basin, southwest of Ireland. Mar. Geol. 188, 193–231.

Delivet, S., 2017. Sedimentary Expression of Internal Waves on Quaternary Contouritic Processes Along the Irish and Moroccan Atlantic Margins. Deparment of Geology. Ghent University, Ghent, Belgium.

Dorschel, B., Wheeler, A.J., Huvenne, V.A.I., de Haas, H., 2009. Cold-water coral mounds in an erosive environmental setting: TOBI side-scan sonar data and ROV video footage from the northwest Porcupine Bank, NE Atlantic. Mar. Geol. 264, 218–229.

Eisele, M., Hebbeln, D., Wienberg, C., 2008. Growth history of a cold-water coral covered carbonate mound — Galway Mound, Porcupine Seabight, NE-Atlantic. Mar. Geol. 253, 160–169.

Eisele, M., Frank, N., Wienberg, C., Hebbeln, D., López Correa, M., Douville, E., Freiwald, A., 2011. Productivity controlled cold-water coral growth periods during the last glacial off Mauritania. Mar. Geol. 280, 143–149.

Flinch, J.F., 1993. Tectonic Evolution of the Gibraltar Arc. Rice University, Houston, Texas, p. 381.

Flinch, J.F., Bally, A.W., Wu, S.G., 1996. Emplacement of a passive-margin evaporitic allochton in the Betic Cordillera of Spain. Geology 24, 67–70.

Fosså, J.H., Lindberg, B., Christensen, O., Lundälv, T., Svellingen, I., Mortensen, P.B., Alvsvåg, J., 2005. Mapping of Lophelia reefs in Norway: experiences and survey methods. In: Freiwald, A., Roberts, J.M. (Eds.), Cold-water Corals and Ecosystems. Springer, Berlin, Heidelberg, pp. 359–391.

Foubert, A., Depreiter, D., Beck, T., Maignien, L., Pannemans, B., Frank, N., Blamart, D., Henriet, J.-P., 2008. Carbonate mounds in a mud volcano province off north-west Morocco: key to processes and controls. Mar. Geol. 248, 74–96.

Frank, N., Ricard, E., Lutringer-Paquet, A., van der Land, C., Colin, C., Blamart, D., Foubert, A., Van Rooij, D., Henriet, J.-P., de Haas, H., van Weering, T., 2009. The Holocene occurrence of cold water corals in the NE Atlantic: implications for coral carbonate mound evolution. Mar. Geol. 266, 129–142.

Frank, N., Freiwald, A., Correa, M.L., Wienberg, C., Eisele, M., Hebbeln, D., Van Rooij, D., Henriet, J.-P., Colin, C., van Weering, T., de Haas, H., Buhl-Mortensen, P., Roberts, J.M., De Mol, B., Douville, E., Blamart, D., Hatté, C., 2011. Northeastern Atlantic cold-water coral reefs and climate. Geology 39, 743–746.

Freiwald, A., 2002. Reef-Forming Cold-Water Corals. In: Wefer, G., Billett, D., Hebbeln, D., Jørgensen, B.B., Schlüter, M., Weering, T.C.E. (Eds.), Ocean Margin Systems. Springer, Berlin, Heidelberg, pp. 365–385.

Freiwald, A., Roberts, J.M., 2005. Cold-water Corals and Ecosystems. Springer, Heidelberg.

Glogowski, S., Dullo, W.C., Feldens, P., Liebetrau, V., Reumont, J., Hühnerbach, V., Krastel, S., Wynn, R.B., Flögel, S., 2015. The Eugen Seibold coral mounds offshore western Morocco: oceanographic and bathymetric boundary conditions of a newly discovered cold-water coral province. Geo-Mar. Lett. 35, 257–269.

de Haas, H., Mienis, F., Frank, N., Richter, T.O., Steinacher, R., Stigter, H., Land, C., Weering, T.C.E., 2009. Morphology and sedimentology of (clustered) cold-water coral mounds at the south Rockall Trough margins, NE Atlantic Ocean. Facies 55, 1–26.

Haines, S.S., Hart, P.E., Collett, T.S., Shedd, W., Frye, M., Weimer, P., Boswell, R., 2017. High-resolution seismic characterization of the gas and gas hydrate system at Green Canyon 955, Gulf of Mexico, USA. Mar. Pet. Geol. 82, 220–237.

Hebbeln, D., Wienberg, C., Beuck, L., Dehning, K., Dullo, C., Eberli, G.P., Freiwald, A., Glogowski, S., Garlichs, T., Jansen, F., Joseph, N., Klann, M., Matos, L., Nowald, N., Reyes, H., Ruhland, G., Taviani, M., Wilke, T., Wilsenack, M., Wintersteller, P., 2012. West Atlantic cold-water coral ecosystems: the west side story - cruise no. MSM20/4 - March 14–April 07, 2012 - Bridgetown (Barbados) - Freetown (Bahamas). In: M.S.M.-B. (Ed.), MSM20/4. DFG-Senatskommission für Ozeanographie, p. 53.

Hebbeln, D., Wienberg, C., Wintersteller, P., Freiwald, A., Becker, M., Beuck, L., Dullo, C., Eberli, G.P., Glogowski, S., Matos, L., Forster, N., Reyes-Bonilla, H., Taviani, M., 2014. Environmental forcing of the Campeche cold-water coral province, southern Gulf of Mexico. Biogeosciences 11, 1799–1815.

Hebbeln, D., Wienberg, C., Bartels, M., Bergenthal, M., Frank, N., Gaide, S., Henriet, J.P., Kaszemeik, K., Klar, S., Klein, T., Krengel, T., Kuhnert, M., Meyer-Schack, B., Noorlander, C., Reuter, M., Rosiak, U., Schmidt, W., Seeba, H., Seiter, C., Strange, N., Terhzaz, L., Van Rooij, D., 2015. In: Merian, Maria S. (Ed.), MoccoMeBo Climate-driven Development of Moroccan Cold-water Coral Mounds Revealed by MeBo-Drilling: Atlantic vs. Mediterranean Settings - Cruise MSM36 - February 18–March 14, 2014 - Malaga (Spain) - Las Palmas (Spain). Berichte, MSM36. DFG-Senatskommission für Ozeanographie, p. 47.

Hebbeln, D., Van Rooij, D., Wienberg, C., 2016. Good neighbours shaped by vigorous currents: cold-water coral mounds and contourites in the North Atlantic. Mar. Geol. 171–185.

Huvenne, V.A.I., De Mol, B., Henriet, J.P., 2003. A 3D seismic study of the morphology and spatial distribution of buried coral banks in the Porcupine Basin, SW of Ireland. Mar. Geol. 198, 5–25.

Huvenne, V.A.I., Bailey, W.R., Shannon, P.M., Naeth, J., di Primio, R., Henriet, J.P., Horsfield, B., de Haas, H., Wheeler, A., Olu-Le Roy, K., 2007. The Magellan mound province in the Porcupine Basin. Int. J. Earth Sci. 96, 85–101.

Huvenne, V.A.I., Van Rooij, D., De Mol, B., Thierens, M., O'Donnell, R., Foubert, A., 2009. Sediment dynamics and palaeo-environmental context at key stages in the Challenger cold-water coral mound formation: clues from sediment deposits at the mound base. Deep-Sea Res. I Oceanogr. Res. Pap. 56, 2263–2280.

Jung, S.J.A., Kroon, D., Ganssen, G., Peeters, F., Ganeshram, R., 2011. Southern Hemisphere intermediate water formation and the bi-polar seesaw. PAGES News 18, 36–38.

Kano, A., Ferdelman, T.G., Williams, T., Henriet, J.-P., Ishikawa, T., Kawagoe, N., Takashima, C., Kakizaki, Y., Abe, K., Sakai, S., Browning, E.L., Li, X., Scientists, Integrated Ocean Drilling Program Expedition 307 Scientists, 2007. Age constraints on the origin and growth history of a deep-water coral mound in the northeast Atlantic drilled during Integrated Ocean Drilling Program Expedition 307. Geology 35, 1051–1054.

Lisiecki, L.E., Raymo, M.E., 2005. A Plio-Pleistocene stack of 57 globally distributed benthic delta 18O records. Paleoceanography 20, PA1003.

Lo Iacono, C., Gràcia, E., Ranero, C.R., Emelianov, M., Huvenne, V.A.I., Bartolomé, R., Booth-Rea, G., Prades, J., Ambroso, S., Dominguez, C., Grinyó, J., Rubio, E., Torrent, J., 2014. The West Melilla cold water coral mounds, Eastern Alboran Sea: morphological characterization and environmental context. Deep-Sea Res. II Top. Stud. Oceanogr. 99, 316–326.

López Correa, M., Montagna, P., Joseph, N., Rüggeberg, A., Fietzke, J., Flögel, S., Dorschel, B., Goldstein, S.L., Wheeler, A., Freiwald, A., 2012. Preboreal onset of cold-water coral growth beyond the Arctic Circle revealed by coupled radiocarbon and U-series dating and neodymium isotopes. Quat. Sci. Rev. 34, 24–43.

Louarn, E., Morin, P., 2011. Antarctic Intermediate Water influence on Mediterranean Sea Water outflow. Deep-Sea Res. I Oceanogr. Res. Pap. 58, 932–942.

Machín, F., Pelegrí, J.L., Marrero-Díaz, A., Laiz, I., Ratsimandresey, A.W., 2006. Near-surface circulation in the southern Gulf of Cádiz. Deep-Sea Res. II Top. Stud. Oceanogr. 53, 1161–1181.

Makou, M.C., Oppo, D.W., Curry, W.B., 2010. South Atlantic intermediate water mass geometry for the last glacial maximum from foraminiferal Cd/Ca. Paleoceanography 25, PA4101.

Maldonado, A., Somoza, L., Pallarés, L., 1999. The Betic orogen and the Iberian-African boundary in the Gulf of Cadiz: geological evolution (central North Atlantic). Mar. Geol. 155, 9–43.

Marchitto, T.M., Broecker, W.S., 2006. Deep water mass geometry in the glacial Atlantic Ocean: a review of constraints from the paleonutrient proxy Cd/Ca. Geochem. Geophys. Geosyst. 7, Q12003.

Matos, L., Mienis, F., Wienberg, C., Frank, N., Kwiatkowski, C., Groeneveld, J., Thil, F., Abrantes, F., Cunha, M.R., Hebbeln, D., 2015. Interglacial occurrence of cold-water corals off Cape Lookout (NW Atlantic): first evidence of the Gulf Stream influence. Deep-Sea Res. I Oceanogr. Res. Pap. 105, 158–170.

Medialdea, T., Vegas, R., Somoza, L., Vázquez, J.T., Maldonado, A., Día-del-Río, V., Maestro, A., Córdoba, D., Fernández-Puga, M.C., 2004. Structure and evolution of the "Olistostrome" complex of the Gibraltar Arc in the Gulf of Cádiz (eastern Central Atlantic): evidence from two long seismic cross-sections. Mar. Geol. 209, 173–198.

Mienis, F., van Weering, T., de Haas, H., de Stigter, H., Huvenne, V., Wheeler, A., 2006. Carbonate mound development at the SW Rockall Trough margin based on high resolution TOBI and seismic recording. Mar. Geol. 233, 1–19.

Mienis, F., de Stigter, H.C., White, M., Duineveld, G., de Haas, H., van Weering, T.C.E., 2007. Hydrodynamic controls on cold-water coral growth and carbonate-mound

development at the SW and SE Rockall Trough Margin, NE Atlantic Ocean. Deep-Sea Res. I Oceanogr. Res. Pap. 54, 1655–1674.
Mienis, F., van der Land, C., de Stigter, H.C., van de Vorstenbosch, M., de Haas, H., Richter, T., van Weering, T.C.E., 2009. Sediment accumulation on a cold-water carbonate mound at the Southwest Rockall Trough margin. Mar. Geol. 265, 40–50.
Mienis, F., De Stigter, H.C., De Haas, H., Van der Land, C., Van Weering, T.C.E., 2012. Hydrodynamic conditions in a cold-water coral mound area on the Renard Ridge, southern Gulf of Cadiz. J. Mar. Syst. 96–97, 61–71.
Moernaut, J., Verschuren, D., Charlet, F., Kristen, I., Fagot, M., De Batist, M., 2010. The seismic-stratigraphic record of lake-level fluctuations in Lake Challa: hydrological stability and change in equatorial East Africa over the last 140 kyr. Earth Planet. Sci. Lett. 290, 214–223.
Picot, M., Droz, L., Marsset, T., Dennielou, B., Bez, M., 2016. Controls on turbidite sedimentation: insights from a quantitative approach of submarine channel and lobe architecture (Late Quaternary Congo Fan). Mar. Pet. Geol. 72, 423–446.
Piper, D., Normark, W., 2009. Processes that initiate turbidity currents and their influence on turbidites: a marine geology perspective. J. Sediment. Res. 79, 347–362.
Pirlet, H., Wehrmann, L.M., Brunner, B., Frank, N., Dewanckele, J.A.N., Van Rooij, D., Foubert, A., Swennen, R., Naudts, L., Boone, M., Cnudde, V., Henriet, J.-P., 2010. Diagenetic formation of gypsum and dolomite in a cold-water coral mound in the Porcupine Seabight, off Ireland. Sedimentology 57, 786–805.
Plassen, L., Vorren, T.O., 2003. Fluid flow features in fjord-fill deposits, Ullsfjorden, North Norway. Nor. J. Geol. 83, 37–42.
Rebesco, M., Hernández-Molina, F.J., van Rooij, D., Wåhlin, A., 2014. Contourites and associated sediments controlled by deep-water circulation processes: state of the art and future considerations. Mar. Geol. 352, 111–154.
Roberts, J.M., 2009. Cold-water coral reefs. In: Steele, J.H., Turekian, K.K., Thorpe, S.A. (Eds.), Encyclopedia of Ocean Sciences, Second edition Academic Press, Oxford, pp. 615–625.
Roberts, J.M., Wheeler, A.J., Freiwald, A., 2006. Reefs of the deep: the biology and geology of cold-water coral Ecosystems. Science 312, 543–547.
Ross, S.W., Rhode, M., Brooke, S., 2017. Deep-sea coral and hardbottom habitats on the west Florida slope, eastern Gulf of Mexico. Deep-Sea Res. I Oceanogr. Res. Pap. 120, 14–28.
Rüggeberg, A., Dullo, C., Dorschel, B., Hebbeln, D., 2007. Environmental changes and growth history of a cold-water carbonate mound (Propeller Mound, Porcupine Seabight). Int. J. Earth Sci. 96, 57–72.
Somoza, L., Ercilla, G., Urgorri, V., León, R., Medialdea, T., Paredes, M., Gonzalez, F.J., Nombela, M.A., 2014. Detection and mapping of cold-water coral mounds and living Lophelia reefs in the Galicia Bank, Atlantic NW Iberia margin. Mar. Geol. 349, 73–90.
Stow, D.A.V., Mayall, M., 2000. Deep-water sedimentary systems: new models for the 21st century. Mar. Pet. Geol. 17, 125–135.
Thierens, M., Browning, E., Pirlet, H., Loutre, M.F., Dorschel, B., Huvenne, V.A.I., Titschack, J., Colin, C., Foubert, A., Wheeler, A.J., 2013. Cold-water coral carbonate mounds as unique palaeo-archives: the Plio-Pleistocene Challenger Mound record (NE Atlantic). Quat. Sci. Rev. 73, 14–30.
Titschack, J., Thierens, M., Dorschel, B., Schulbert, C., Freiwald, A., Kano, A., Takashima, C., Kawagoe, N., Li, X., 2009. Carbonate budget of a cold-water coral mound (Challenger Mound, IODP Exp. 307). Mar. Geol. 259, 36–46.
Titschack, J., Baum, D., De Pol-Holz, R., López Correa, M., Forster, N., Flögel, S., Hebbeln, D., Freiwald, A., 2015. Aggradation and carbonate accumulation of Holocene Norwegian cold-water coral reefs. Sedimentology 62, 1873–1898.
Van der Land, C., Mienis, F., De Haas, H., Frank, N., Swennen, R., Van Weering, T.C.E., 2010. Diagenetic processes in carbonate mound sediments at the south-west Rockall Trough margin. Sedimentology 57, 912–931.
Van Rensbergen, P., Depreiter, D., Pannemans, B., Henriet, J.-P., 2005a. Seafloor expression of sediment extrusion and intrusion at the El Arraiche mud volcano field, Gulf of Cadiz. J. Geophys. Res. Earth Surf. 110, F02010.
Van Rensbergen, P., Depreiter, D., Pannemans, B., Moerkerke, G., Van Rooij, D., Marsset, B., Akhmanov, G., Blinova, V., Ivanov, M., Rachidi, M., Magalhaes, V., Pinheiro, L., Cunha, M., Henriet, J.-P., 2005b. The El Arraiche mud volcano field at the Moroccan Atlantic slope, Gulf of Cadiz. Mar. Geol. 219, 1–17.
Van Rooij, D., Versteeg, W., the CADIPOR II shipboard scientific party, 2005. Cruise Report Belgica 05/12 "CADIPOR II", Gulf of Cadiz, off Larache, Morocco. RCMG Internal Publication (43 pp).
Van Rooij, D., Blamart, D., Richter, T., Wheeler, A., Kozachenko, M., Henriet, J.P., 2007. Quaternary sediment dynamics in the Belgica mound province, Porcupine Seabight: ice-rafting events and contour current processes. Int. J. Earth Sci. 96, 121–140.
Van Rooij, D., Iglesias, J., Hernández-Molina, F.J., Ercilla, G., Gomez-Ballesteros, M., Casas, D., Llave, E., De Hauwere, A., Garcia-Gil, S., Acosta, J., Henriet, J.P., 2010. The Le Danois Contourite Depositional System: interactions between the Mediterranean Outflow Water and the upper Cantabrian slope (North Iberian margin). Mar. Geol. 274, 1–20.
Van Rooij, D., Blamart, D., De Mol, L., Mienis, F., Pirlet, H., Wehrmann, L.M., Barbieri, R., Maignien, L., Templer, S.P., de Haas, H., Hebbeln, D., Frank, N., Larmagnat, S., Stadnitskaia, A., Stivaletta, N., van Weering, T., Zhang, Y., Hamoumi, N., Cnudde, V., Duyck, P., Henriet, J.P., 2011. Cold-water coral mounds on the Pen Duick Escarpment, Gulf of Cadiz: the MiCROSYSTEMS project approach. Mar. Geol. 282, 102–117.
Vandorpe, T., Van Rooij, D., de Haas, H., 2014. Stratigraphy and paleoceanography of a topography-controlled contourite drift in the Pen Duick area, southern Gulf of Cádiz. Mar. Geol. 349, 136–151.
Vandorpe, T., Martins, I., Vitorino, J., Hebbeln, D., García, M., Van Rooij, D., 2016. Bottom currents and their influence on the sedimentation pattern in the El Arraiche Mud Volcano Province, southern Gulf of Cadiz. Mar. Geol. 378, 114–126.
Wainer, I., Goes, M., Murphy, L.N., Brady, E., 2012. Changes in the intermediate water mass formation rates in the global ocean for the Last Glacial Maximum, mid-Holocene and pre-industrial climates. Paleoceanography 27, PA3101.
van Weering, T.C.E., de Haas, H., de Stigter, H.C., Lykke-Andersen, H., Kouvaev, I., 2003. Structure and development of giant carbonate mounds at the SW and SE Rockall Trough margins, NE Atlantic Ocean. Mar. Geol. 198, 67–81.
Wheeler, A.J., Beyer, A., Freiwald, A., de Haas, H., Huvenne, V.A.I., Kozachenko, M., Olu-Le Roy, K., Opderbecke, J., 2007. Morphology and environment of cold-water coral carbonate mounds on the NW European margin. Int. J. Earth Sci. 96, 37–56.
Wienberg, C., Titschack, J., 2017. Framework-Forming Scleractinian Cold-Water Corals through Space and Time: A Late Quaternary North Atlantic Perspective. In: Rossi, S., Bramanti, L., Gori, A., Orejas, C. (Eds.), Marine Animal Forests: The Ecology of Benthic Biodiversity Hotspots. Springer International Publishing, Switzerland.
Wienberg, C., Hebbeln, D., Fink, H.G., Mienis, F., Dorschel, B., Vertino, A., Correa, M.L., Freiwald, A., 2009. Scleractinian cold-water corals in the Gulf of Cádiz—first clues about their spatial and temporal distribution. Deep-Sea Res. I Oceanogr. Res. Pap. 56, 1873–1893.
Wienberg, C., Frank, N., Mertens, K.N., Stuut, J.-B., Marchant, M., Fietzke, J., Mienis, F., Hebbeln, D., 2010. Glacial cold-water coral growth in the Gulf of Cádiz: implications of increased palaeo-productivity. Earth Planet. Sci. Lett. 298, 405–416.
Zitellini, N., Gràcia, E., Matias, L., Terrinha, P., Abreu, M.A., DeAlteriis, G., Henriet, J.P., Dañobeitia, J.J., Masson, D.G., Mulder, T., Ramella, R., Somoza, L., Diez, S., 2009. The quest for the Africa-Eurasia plate boundary west of the Strait of Gibraltar. Earth Planet. Sci. Lett. 280, 13–50.